Thermal condensations in large stellar coronal loops

J.M. Ferreira[1] **and C.A. Mendoza-Briceño**[2]

[1] Department of Physics and Astronomy, University of St. Andrews, St. Andrews KY16 9SS, Scotland
[2] Centro de Astrofísica Teórica, Facultad de Ciencias, Universidad de los Andes, Mérida, Venezuela

Abstract. The equations ruling the thermal equilibrium along coronal loops on rapidly rotating solar-type stars are solved. The particular case of loops with lengths comparable or greater than a stellar radius is studied.

Depending on the base pressure, it is found that hot loops can exist either with very high coronal temperature ($T \sim 10^7$ K) or with a more solar like temperature ($T \sim 10^6$ K). Another type of solution consist of loops with a local temperature minimum at the summit which can be thought as representing a stellar slingshot prominence. A detailed study is presented and it is shown that these solutions are available in very general circumstances and without any special requirements such as those concerning the heating distribution along the loop or variations of the cross-sectional area.

The equilibrium structure of asymmetric loops is analysed. The maximum temperature of hot loops moves towards the loop leg with more heating, but surprisingly, depending on the parameters of the problem, the prominence solution can appear in either loop leg.

Key words: stars: magnetic fields – stars: coronae – plasmas

1. Introduction

A lot of effort has been made towards understanding the thermal structure of the observed solar coronal loops. The existence of hot loops ($T \gtrsim 10^6$ K) has been explained with considerable success by static models (Rosner et al. 1978; Serio et al. 1981; Vesecky et al. 1979). An intriguing feature comes from the observations of the Sun in optically thin UV and EUV lines. The emission measure has a minimum at $T \sim 10^5$ K, a characteristic not reproduced by standard loop models. The explanation may lie in the fact that under certain circumstances there is a cool loop solution of the energy equation besides the usual hot one (Hood & Priest 1979; Martens & Kuin 1982). These solutions are possible only for short loops and have temperatures of less than 80000 K along their entire length. Antiochos & Noci (1986)

argue that an ensemble of cool and hot loops can account for this observed rise in the emission measure at low temperatures. The success of this thesis relies upon the existence of short cool loops which depends critically on the exact form of the cooling function for optically thin plasmas as well as the heating distribution along the loop.

In a seminal paper Hood & Anzer (1988, HA) presented analytical solutions to approximate equations of thermal equilibrium and showed, using the powerful method of phase-plane analysis, the possibility of hot, cool and hot-cool solutions. The latter ones are similar to hot loops but have a small and very cold region at the loop summit. These are extremely interesting solutions and can be thought as representing coronal condensations, i.e., prominences, in thermal and hydrostatic equilibrium. Numerical solutions of the exact equations have been obtained in a series of papers by Steele & Priest (1990, 1991, 1994), where they investigate in detail the influence of gravity and a loop area expansion on the type of solutions available. In the presence of a realistic solar gravity no hot-cool solutions were found, although the authors suggest that incorporating a loop area expansion will make these solutions available. Recently, Mendoza (1996) has been able to show the existence of hot-cool solutions for constant area loops in the presence of gravity when a spatially dependent heating function is employed.

The X-ray spectra of active and rapidly-rotating late-type stars are usually well fitted by a two component thermal plasma, one with $T \sim$ few $\times 10^6$ K and the other with $T \sim$ few $\times 10^7$ K. This high temperature component plasma can either be due to stellar-sized or to relatively small but very high pressure loops as suggested by the well known scaling laws of constant pressure loops $T_{\max} \propto (Lp)^{1/3}$. Independent evidence for the existence of very large magnetic loops on these stars comes from the discovery of stellar slingshot prominences suspended several stellar radii above the surface (Collier Cameron & Robinson 1989a,b). These cool clouds lie above the Keplerian co-rotation radius and move in solid-body rotation with the star which strongly suggests the presence of large closed magnetic loops to support them against centrifugal ejection. Stellar slingshot prominences are not a feature of a particular star but rather a very common property in rapidly-rotating active single stars (Collier Cameron 1996) and probably of close binary stars (e.g.

Steeghs et al. 1996). Moreover, eclipsing binary systems show the presence of an extended and very hot corona supporting the idea that 10^7 K stellar-sized loops exist on these systems. A relevant fact is the non-existence of a solar analogue to either the stellar-sized prominence loop structures or to the very high temperature loops. However, one has to be sceptical in accepting *prima facie* the existence of the very hot and large stellar loops in single stars as it is also possible that this high temperature component could arise from compact and short flaring loops, more akin to what is observed on the Sun. In this alternative scenario, the extended very hot corona is a particular property of some active binaries that is not extendable to single systems and the large loops on single stars are likely to have a solar-like temperature.

Collier Cameron (1988) (hereafter CC88) calculated thermal equilibrium models for large stellar coronal loops in rapidly rotating systems. As in previous works on solar loops (Serio et al. 1981, Vesecky et al. 1979), he finds two types of solutions. One with a temperature maximum at the loop summit and another one with a local temperature minimum. The loop temperature and density obtained are consistent with those estimated from observations if one assumes that the large and very hot loops are real. The results are also in reasonable agreement with the simple scaling laws for constant pressure loops. Although loops with a temperature inversion near the summit were found, their temperature was much too high to resemble prominence solutions. Loops with varying cross-sectional area were also studied but the results are largely influenced by the particular form of the heating function chosen (cf. Sect. 8). Recently, van den Oord & Zuccarello (1996) have revisited this problem from a qualitative point of view in a manner similar to HA. They argue that the solutions of CC88 with a temperature inversion near the summit in a loop with constant cross-sectional area and in the presence of a realistic gravity do not exist but become possible for expanding loops.

The purpose of the present paper is to revisit by means of a numerical approach the problem of thermal equilibrium with focus on large coronal loops of rapidly-rotating stars. This allows us to use loops with physical area variations, several different forms of the heating function, gravity variations along the field and also to study asymmetries with respect to the loop summit. In Sects. 2 & 3 we present the problem and equations to be solved. We then analyse the effects of an exponential decreasing heating and of an area variation along the loop (Sect. 4). Next, we present solutions and study their dependence on the parameters (Sects. 5 & 6). In Sect. 7 we investigate the nature of asymmetric loops and in particular how this affects condensation-type solutions. Finally, in Sect. 8 we discuss the implications of our results and summarize in Sect. 9.

2. Physical considerations

Let us consider a certain magnetic field configuration in static equilibrium embedded in a co-rotating stellar atmosphere and denote the plasma pressure, density and temperature by P, ρ and

T respectively. The plasma along a field line will distribute itself according to the momentum equation projected in that direction

$$\frac{dp}{ds} = \rho g_{e_\parallel}, \tag{1}$$

where s is the coordinate along a particular field line and $g_{e_\parallel}$ represents the joint gravitational and centrifugal forces projected along the field.

In static equilibrium, force balance must also occur in the directions perpendicular to the field, but we will consistently ignore this by taking the field lines as rigid and unperturbed by the other forces. The effect of the magnetic field is mainly a passive one. It has the ability to channel heat conduction predominantly along its direction and therefore, the conductivity tensor κ, is very anisotropic and in general $k_\parallel \gg k_\perp$ (Spitzer 1962). This simplifies the energy equation to

$$\frac{1}{A} \frac{d}{ds}(Ak_\parallel \frac{dT}{ds}) = C - H, \tag{2}$$

where C represents the cooling mechanisms, H the heating sources, $A(s)$ is the cross-sectional area of a flux tube and $\kappa_\parallel = K_0 T^{\frac{5}{2}}$, with $K_0 = 10^{-11}$ Wm^{-1}K$^{-7/2}$ a constant.

2.1. The heating function

The exact mechanisms that heat stellar coronae are unknown, but there is a large consensus that the heating is of magnetic origin. Generally, one can consider $H = H(\rho, T, B, s, ...)$, with the dependence on the different parameters varying according to the particular heating mechanism considered. The simple forms $H = h'\rho$ or $H = h$, with h and h' constants, are often used. In the first case it is assumed that each particle receives the same amount of energy, while in the second, it is assumed instead a constant heat per unit volume. The justification for using these type of functions lies primarily in their simplicity.

Other authors (e.g. Rosner et al. 1978; Serio et al. 1981) have adopted a spatially dependent heating function of the type $H = h \exp(-s/s_h)$, where s_h is the heating deposition scale height. In his study of the thermal properties of stellar coronal loops, CC88 adopts a function of the form $H = \left[h/A(s)\right] \exp(-s/s_h)$, constrained by the condition that the total heating deposited in the loop, $H_t = \int A(s)H ds$, remains the same for loops of different heights and different area expansions.

For prominence-like condensations other physical effects become relevant. The density changes almost discontinuously from the corona to the prominence, causing waves to reflect and giving a reduced wave heating inside the prominence. On the other hand, the low prominence temperature can increase the reconnection rates by a considerable amount due to an increase in the magnetic diffusivity η (Steinolfson & van Hoven 1984), giving rise to an increased heating inside the prominence.

Whatever function one decides to use, one must ascertain the dependence of the results on the type of function chosen. For example, the temperature structure of hot loops is known to have very little dependence on the heating function (e.g. Rosner et al. 1978; Unruh & Jardine 1996). We find it wiser to concentrate all

our ignorance in only one spatially dependent function and so we choose $H = h \exp(-s/s_{\mathrm{h}})$. In Sect. 6.4 we investigate other forms of heating functions to show that the main features of our results are not an artifact of the particular phenomenological heating function we have adopted.

2.2. The cooling function

The plasma cools by radiation and for an optically thin plasma one can take $C = \rho^2 Q(T)$, where $Q(T)$ is the cooling function. This function is dependent on the element abundances, which vary both from star to star and from the photosphere to the corona on the same star. Most of the available cooling functions were determined using cosmic abundances (e.g. Cox & Tucker 1969; Raymond & Smith 1977; McClymont & Canfield 1983), although Cook et al. (1989) have performed a calculation for solar coronal abundances and found that the function's peak moves to slightly higher temperature. Bearing in mind that our interest is focused on other stars of unknown coronal chemical composition, it is reasonable to consider a cooling function based on cosmic abundances. Also, the exact shape of the cooling function is only important for the short cool loop solutions which we will not consider. The effect of opacity on the radiative losses depends not only on temperature but also on pressure, geometrical effects and the radiation field in which it is immersed and so requires the solution of the complete radiative transfer problem. Kuin & Poland (1991) find that the optically thin approximation overestimates the radiative losses for $T < 4 \times 10^4$ K , with optical thickness dominant for $T < 1.3 \times 10^4$ K.

In the same spirit of other works, we consider the plasma to be optically thin and use the analytical fit of Hildner (1974) extended to higher temperatures according to CC88. This keeps the problem treatable, but we will bear in mind that such simplification may influence the results.

2.3. The loop shape

Let us consider a symmetric loop with a given length. Its shape determines the value of gravity projected along the field which has a direct influence on the pressure distribution. Throughout this work we will consider the simple case of a dipole oriented parallel to the rotation axis and located at the centre of the star. With this choice, the relation between s, the coordinate along the field line, and the spherical coordinates is

$$r \frac{d\theta}{ds} = \frac{B_\theta}{B} = \frac{\sin\theta}{\sqrt{1 + 3\cos^2\theta}}. \tag{3}$$

For a loop with maximum height r_m, the footpoint is at $\theta_0 = \arcsin(\sqrt{R_\star/r_{\mathrm{m}}})$ and integrating Eq. (3) gives the relation between θ and s. With this choice, the effective gravity along the field is given by the expression

$$g_{e_\parallel} = -\frac{2\cos\theta}{\sqrt{(1 + 3\cos^2\theta)}}\left(\frac{GM_\star}{r^2} - \frac{3}{2}\omega^2 r \sin^2\theta\right), \tag{4}$$

where $M_\star$ represents the stellar mass, ω the stellar angular velocity and G the the gravitational constant. The function $g_{e_\parallel}$ becomes zero at the loop summit and also whenever

$r^3 = 2GM_\star/3\omega^2 \sin^2\theta$, these last points we denote as the effective corotation radius ($R_{\kappa e}$).

Observations have shown that the area of solar magnetic loops can either be almost uniform or vary significantly along its length (e.g. Klimchuk et al. 1992) and by analogy one expects a similar behaviour for stellar loops. Unfortunately, there are very few analytical force-free field solutions known that could be used to simulate the different types of loop area expansion, so that, in order to understand the influence of area expansion on the solutions of thermal equilibrium, we have adopted the simple approach of fixing the shape of the loop to be that of a dipole but prescribe the area variation independently. We follow CC88 and parameterise $A = r^x$, with x a free parameter of the problem.

3. The equations and their boundary conditions

For a fully ionized H plasma the momentum and energy equations take the form

$$\frac{dp}{ds} = \rho g_{e_\parallel} \tag{5}$$

$$\rho^2 Q(T) - H - \frac{1}{A}\frac{d}{ds}(AK_0 T^{\frac{5}{2}}\frac{dT}{ds}) = 0, \tag{6}$$

with $p = 2\rho RT$ and the cooling as piecewise function of the form $Q(T) = \chi T^\alpha$. It is convenient to use dimensionless equations. For this purpose let us set $p = p_0\overline{p}$, $T = T_0\overline{T}$, $s = R_\star\overline{s}$, $s_{\mathrm{h}} = R_\star\overline{s_{\mathrm{h}}}$, $r = R_\star\overline{r}$ and $A = A_0\overline{A}$.
Our equations then become

$$\frac{d\overline{p}}{d\overline{s}} = \frac{\overline{p}}{\overline{T}}\overline{g} \tag{7}$$

$$\frac{1}{\overline{A}}\frac{d}{d\overline{s}}(\overline{A}\,\overline{T}^{\frac{5}{2}}\frac{d\overline{T}}{d\overline{s}}) = \xi\left(\frac{\overline{p}^2}{\overline{T}^2}\overline{T}^{\overline{\alpha}}\overline{\chi} - \overline{H}\right) \tag{8}$$

where

$$\xi = \frac{R_\star^2 \chi_0 p_0^2 T_0^{\alpha_0 - \frac{11}{2}}}{4K_0 R^2}, \qquad \overline{H} = he^{-\overline{s}/\overline{s_{\mathrm{h}}}}\frac{4R^2}{p_0^2\chi_0 T_0^{\alpha_0-2}}, \tag{9}$$

$$\overline{g} = g_{e_\parallel}\frac{R_\star}{2T_0 R}, \qquad \overline{T}^{\overline{\alpha}}\overline{\chi} = \frac{T^\alpha \chi}{T_0^{\alpha_0}\chi_0}. \tag{10}$$

We choose $T_0 = 10^5$ K, a temperature at which the cooling function has its maximum, and $p_0 = 1$ pa, as inferred from observations when assuming that the high temperature component comes from large loops (e.g. Collier Cameron et al. 1988). Since the stars we are interested are relatively similar to the Sun we take $R_\star = R_\odot$ and $M_\star = M_\odot$. In what follows we shall always refer to the dimensionless quantities and so we drop the overline from all the variables.

The solution of these system of equations requires the specification of three boundary conditions. Choosing the correct boundary conditions is important and has been subject of intensive discussion in the literature (for a comprehensive overview

please refer to HA). On the lower boundary we adopt a chromospheric temperature $T_b = 0.2$ which is still high enough that Eq. (6) can be representative of the physics of the problem. For the other lower boundary condition we can either choose to fix the conductive flux or the base pressure. CC88 chose to fix the value of the conductive flux based on the knowledge of the differential emission measure in the CIV resonance lines. However, this gives information on the values averaged over the stellar surface and we believe that it does not put any real constraint on the flux at the base of a particular loop. From experiment we found that there was no real difference between fixing the base pressure or the base flux. We choose to fix the pressure and obtain the thermal flux as an output for computational reasons. The last condition is that the loop is symmetric about the summit, i.e., $dT/ds = 0$ there.

Finally, let us summarize the parameters of our problem: base pressure (p), area expansion rate (x), base heating (h), heating deposition length-scale (s_h) and stellar angular velocity (w).

4. Qualitative effects

We can rewrite Eqs. (7, 8) in the form of first order differential equations

$$\frac{dp}{ds} = \frac{p}{T}g \tag{11}$$

$$\frac{dT}{ds} = \frac{F_c}{A}T^{-\frac{5}{2}} \tag{12}$$

$$\frac{dF_c}{ds} = A\xi\left(p^2\chi T^{\alpha-2} - H\right). \tag{13}$$

The right-hand side of the energy related equations is explicitly dependent on s due to A, H, and p. By considering the simple case of constant area, constant heating and zero gravity, our system of equations becomes autonomous and easier to analyse (HA). With $A \propto \exp(s)$ the above set of equations are still autonomous which allows a relatively easy analysis (van den Oord & Zuccarello 1996). But one must bear in mind that with this area profile the maximum rate of expansion occurs at the loop summit while in a realistic symmetric magnetic loop $dA/ds = 0$ there, so that this prescription is only qualitatively acceptable.

A detailed study of the solutions (e.g. determination of summit temperature and loop length in function of the parameters) requires the numerical solution of Eqs. (12, 13) (Steele & Priest 1990), but we will avoid this and proceed to consider the influence of a spatially dependent heating in the solutions.

4.1. Spatially dependent heating function

Let us analyse the case of a spatially dependent heating function, $H = h\exp\left(-s/s_h\right)$, while maintaining the assumptions of constant area and zero gravity.

Our equation has the form

$$\frac{d}{ds}(T^{\frac{5}{2}}\frac{dT}{ds}) = \xi'(\chi T^{\alpha-2} - \frac{h}{p^2}e^{-\frac{s}{s_h}}) \tag{14}$$
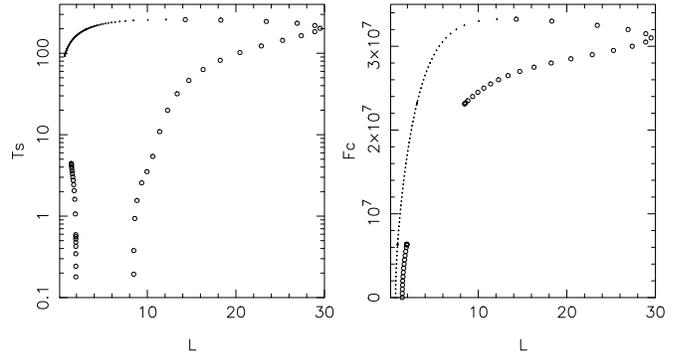

Fig. 1. The solutions for the case $g = 0$, $x = 0$, $p = 1$ and a spatially dependent heating, $H = h\exp\left(-s/s_h\right)$, with $h = 10^{-5}$ and $s_h = 2.5$. The summit temperature and base flux are shown as a function of the loop half-length. Open circles represent solutions with a local temperature minimum at the summit while dots represent solutions with the maximum occurring at the summit.

with $\xi' = \xi p^2$ (Mendoza and Hood, 1996). Let us first note that because the right-hand side is explicitly dependent on s, our second order ordinary differential equation (o.d.e.) is nonautonomous, and neither are there critical points nor can we define a separatrix curve. This equation constitutes a two-point boundary value problem, but can actually be solved as a simple o.d.e. without any iteration procedure. For a given base flux, with h/p^2, ξ' and s_h fixed, we integrate from the origin until $dT/ds = 0$. This defines a hot solution with a certain length L_1. If we continue integrating from this point onwards we can either find $dT/ds = 0$ for the second time, defining a hot-cool solution with a greater length L_2, or that the temperature goes to zero while the flux does not approach the T-axis, i.e., in some sense the contour is outside the 'separatrix' and no hot-cool solution exists. In principle, we could continue integrating after L_2 in order to find $dT/ds = 0$ for the third time and so on, but the solutions thus obtained seem to be rather unphysical.

A particular case is presented in Figs. 1 & 2. Fig. 2 represents some of the solutions in the phase-plane (Fc, T). Every solution must start at $T = T_b$ and finish at $dT/ds = 0$ (i.e. at the x-axis). The first thing to notice is the lack of symmetry of the phase-plane with respect to the T-axis, an obvious consequence of the s-dependence of the heating. For a given base flux this has the effect of making both the hot and hot-cool solutions, when available, hotter and longer than when the heating is constant. If we compare instead solutions with the same length a spatially decreasing heating function gives rise to cooler hot solutions with smaller base flux, as one would have intuitively predicted.

For a certain range of fluxes there are no hot-cool solutions available (e.g. dash-dot-dot-dot line in Fig. 2; this corresponds to the existence of a gap for the hot-cool solutions in Fig. 1), but if the base flux increases above a given value, we recover this type of solutions (e.g. solid line). As one would intuitively expect, a reduction in the heating can lead to condensations by turning open contours into closed ones. Increasing the base flux even further causes the temperature of the hot-cool solution to
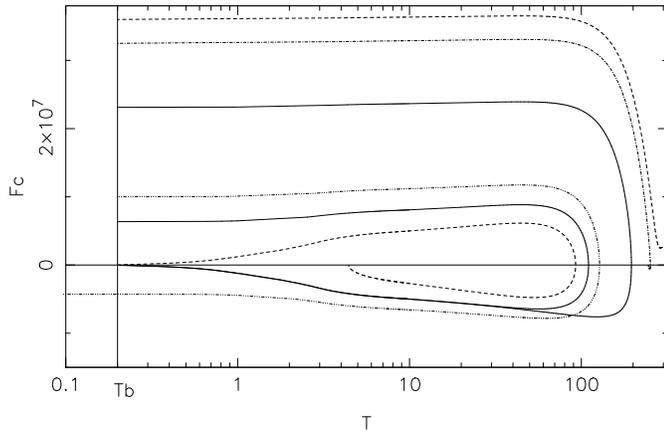
Fig. 2. Some representative solutions in the phase-plane for the case shown in Fig. 1. Prominence solutions exist for low and high flux (solid line) while for intermediate flux no hot-cool solutions exist (dash-dot-dot-dot line). For very high flux only small temperature inversions are possible (dash-dot line). Above a critical flux no solutions exist (dashed line).

increase until it equals the one of the hot solution (dash-dot line). In reality, these hot-cool loop solutions have no longer a cool apex although we maintain this terminology just to emphasise that they have a local temperature minimum at the summit. Above a critical flux neither hot nor hot-cool solutions exist (e.g dashed line). This also defines the maximum length of a hot solution. For longer loops a hot solution is not possible because it cannot obey the condition that results from having a maximum temperature at the summit,

$$\frac{h}{p^2}e^{-\frac{s}{s_h}} > \chi T^{\alpha-2}. \tag{15}$$

This is in contrast with the case of constant heating for which no limit exist on the length of hot loops (cf. Steele & Priest 1990).

The results obtained so far allow us to interpret some of the conclusions made by CC88. Namely, the existence of a maximum loop length and the existence of hot loops with and without local temperature minima, are a direct consequence of the spatially dependent heating function adopted. (Although we do not impose the total heating, $H_t = \int h \exp\left(-s/s_h\right) A ds$, to be the same for loops of different lengths as in CC88, this has no influence on our conclusions as for $L \gg s_h$, $H_t \approx h s_h$, independent of the loop length.) The fact that CC88 did not find prominence-like solutions is a consequence of the parameter space explored (Sect. 6).

4.2. The effect of gravity and area variation

The effects of gravity and area variation can be better understood by a qualitative analysis. For a variable cross-sectional area the energy equation can be written as follows

$$\frac{d}{ds}\left(T^{\frac{5}{2}}\frac{dT}{ds}\right) = \xi\left(C - H\right) - \frac{1}{A}\frac{dA}{ds}\frac{dT}{ds}T^{\frac{5}{2}}. \tag{16}$$
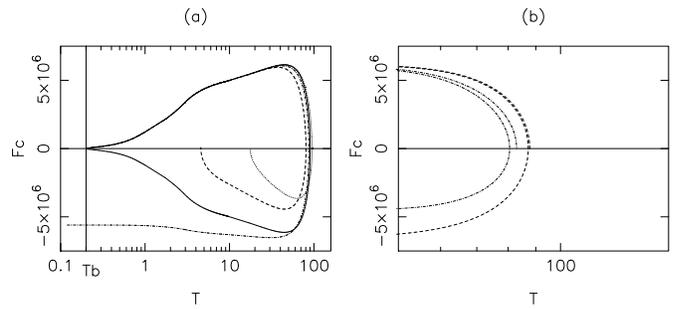

Fig. 3a and b. The influence of the different effects on the phase-plane for the solution with zero flux. **a** Hot-cool solutions. Cases shown are: zero gravity and constant heating (solid line), area variation with $x = 2$ (dashed line), spatial dependent heating with $s_h = 1.5$ (dotted line) and gravity (dot-dash line). **b** Zoom at the hottest part of the phase-plane for hot and hot-cool solutions in the presence of gravity (dot-dash line) and area variation (dashed line).

An area increase works as an extra heating source if $dT/ds > 0$ or as an extra cooling if $dT/ds < 0$. In other words, the absolute value of the conductive flux decreases and open contours in the phase-plane can change to close contours.

The effect of gravity is to decrease the cooling due to the decrease in the pressure and so has the opposite effect of a decaying heating, tending to turn closed contours into open ones.

These effects are illustrated in the phase-plane where the zero flux solution is shown with the several different effects being included separately (Fig. 3). Gravity tends to suppress the hot-cool solutions, while an area variation or a spatially dependent heating favour the existence of this type of solutions. These general properties of the hot-cool solutions were first determined by HA. For long enough loops the effective gravity changes sign at $R_{\kappa e}$ and the increase in pressure also favours the closure of the contours in the phase-plane, i.e., it can lead to condensations (cf. Sect. 6.3).

It is important to realise that, in the presence of gravity or area variation, a contour in the phase-plane that reaches zero flux does not automatically define a solution. At the summit one has the additional conditions $g = 0$ and $dA/ds = 0$. This has two important implications. Firstly, the solutions have to be found using iterative procedures. Secondly, the first time the contour of a hot-cool solution crosses $dT/ds = 0$ does not define a solution as illustrated in Fig. 3b.

5. A typical solution

Due to the large parameter space we choose to study in detail the properties of the solutions for a particular case for which we take typical values of the parameters. We refer to these solutions as the standard solutions. Let us take for the parameters of our problem $h = 10^{-5}$, $s_h = 1.5$, $p = 1.0$, $x = 2$ and $\omega = 1.4 \times 10^{-4}$ s (corresponding to a star with a rotation period $P_{rot} \approx 0.5$ d). The solutions available are represented in Fig. 4. It is clear that for this set of parameters there are no hot-cool solutions for low base thermal flux because gravity turns closed contours in the
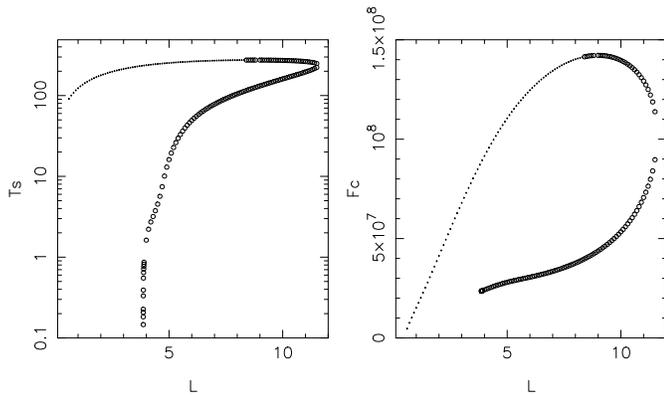
Fig. 4. Summit temperature and base flux versus loop half length for solutions of the standard case. The parameter used are $h = 10^{-5}$, $s_h = 1.5$, $x = 2$, $p = 1.0$. Open circles represent solutions with a local temperature minimum at the summit and dots represent solutions with the maximum occurring at the summit.

Fig. 5. Temperature and gas pressure from the loop base to the summit for some selected solutions of the standard case. The parameters used are $h = 10^{-5}$, $s_h = 1.5$, $x = 2$, $p = 1.0$ and $\omega = 1.4 \times 10^{-4}$. The solutions shown have: $L = 3.87$, $Fc = 2.4 \times 10^7$ (full line); $L = 3.87$, $Fc = 8.9 \times 10^7$ (dashed line); $L = 10.0$, $Fc = 5.3 \times 10^7$ (dash-dotted line) and $L = 10.0$, $Fc = 1.4 \times 10^8$ (dotted line). The symbol $\times$ shows the position of $R_{\kappa e}$ along the loop for the different solutions.

phase-plane into open ones. However, for higher flux and longer length, condensations are possible due to the influence of the area variation, the decaying heating and the increase in pressure due to the change in sign in g. As established in the previous section, one of the repercussions of the adopted heating function is the existence of a critical length above which there are no available solutions. Also, beyond a certain length there are no hot loops but only hot-cool loops with high summit temperatures.

The temperature and pressure variation along the loop for some characteristic solutions is shown in Fig. 5. A hot-cool and a hot solution with the same length, $L = 3.87$ (corresponding to a loop whose summit lies $\sim 2.5\,R_*$ above the stellar surface), are shown for comparison. At the summit the area is about 12 times larger than the area at the base, and the heating about 13 times lower. The solution representing a condensation has a base flux about four times lower than the respective hot solution. The hot-cool solution has a coronal temperature over most of its length with sharp transition regions at the footpoints and at the summit. Its maximum temperature occurs closer to the footpoints and it is about half the maximum temperature of the hot solution. The gas pressure variation is not very pronounced although the variation is larger for the hot-cool solution due to the smaller pressure scale-height. Despite the fact that the pressure variation is small, it still has an important effect on the available solutions.

At the summit, the decrease in temperature from coronal values to chromospheric values takes place in a very narrow interval. The temperature decrease from 70.0 to 0.2 occurs in the interval $\Delta L = 0.2$ and from 10 to 0.2 in the interval $\Delta L = 3 \times 10^{-4}$. Integrating the density along the loop for both hot-cool and hot solutions gives for the ratio of their masses, $m_{h-c}/m_h = 1.6$. The extra mass of the hot-cool solution is a significant fraction of the total mass contained in the hot loop, suggesting that a considerably large amount of plasma must be driven from the surface to the loop summit to supply its mass.
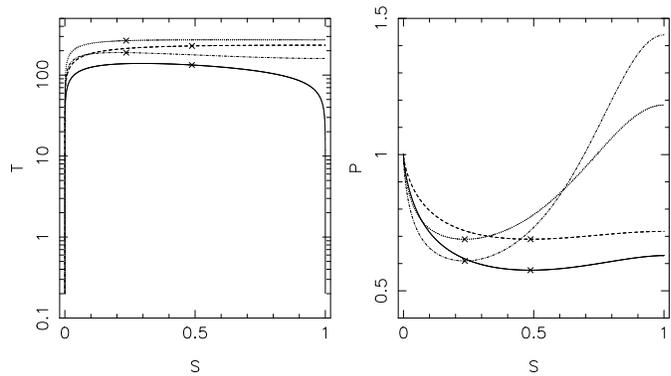
Two other solutions are shown with $L = 10.0$ and having a local temperature minimum at their summits. The dotted line represents a solution with a base flux, summit temperature and maximum temperature higher than the solution shown as dash-dotted. The former solution also has an extremely small temperature inversion. The gas pressure for both solutions reaches values higher than the base pressure because they lie much above $R_{\kappa e}$.

6. Dependence on the parameters

In this section we examine the dependence of the available solutions on the different parameters. Intuitively, we expect that varying parameters as to increase the cooling, or to decrease the heating, will lead more easily to condensations and to cooler and shorter hot solutions, and vice-versa.

6.1. Variation with heating deposition length-scale

For a constant heating, i.e. $s_h = \infty$, there are no hot-cool solutions if we keep the other parameters unchanged. However, for slightly different parameters, hot-cool solutions exist but only for the lower length branch of solutions, as shown in Fig. 6. This a natural result since the longer length branch is in essence a result of the spatial decaying heating if the rate of area increase is not very large and the centrifugal component of g not very important due to the very high temperature of the corona. We were unable to find a maximum loop length, a predictable consequence of taking a constant heating (cf. Sect. 4.1). However, we suspect it might exist for very long lengths as a result of the induced increase in cooling caused by the increase of gas pressure with height after $R_{\kappa e}$ (cf. Sect. 6.3).

A decrease in s_h, leads to a decrease of the heating with height which allows for the existence of two branches of condensation type solutions (Fig. 6b). However, if it decreases be-
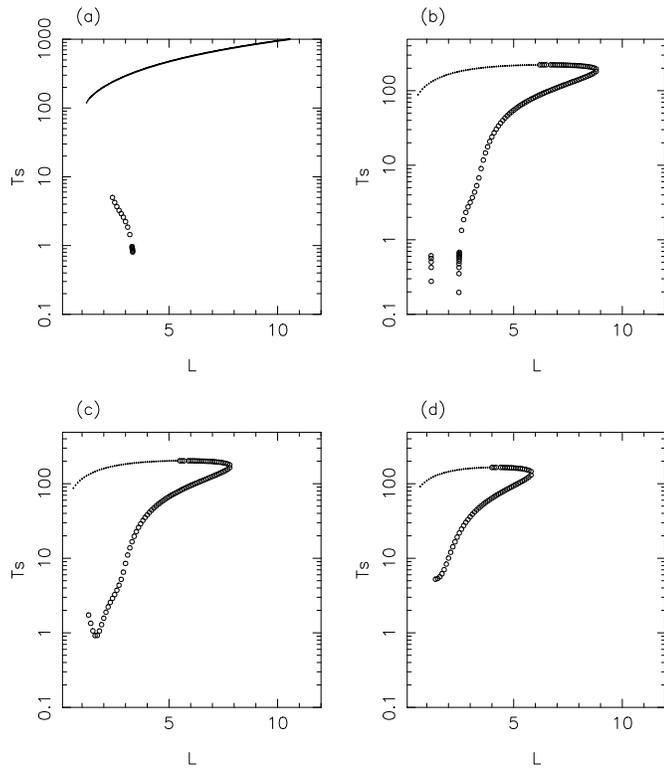
Fig. 6a–d. The solutions' dependence on s_h. All other parameters are the standard ones with the exception of case (a): **a** For $h = 0.5 \times 10^{-5}$, $s_h = \infty$, $x = 3$ and $p = 2.0$; note the different scale of the y-axis, the very high temperature hot solutions are only represented for completeness but are unphysical; **b** $s_h = 1.15$; **c** $s_h = 1.03$; **d** $s_h = 0.8$

Fig. 7a and b. The solutions' dependence on area expansion rate: **a** $x = 0$; **b** $x = 5$. All the other parameters are the same as for the standard case. Notice the different scaling of the axis for case **b** and the unphysical nature of the very hot long loops.

Fig. 8a and b. The solutions' dependence on p, h and g_{eff}: $p = 0.025$ and $h = 5.0 \times 10^{-8}$; **a** the other parameters are the standard ones; **b** $x = 0$, $s_h = \infty$ and $\omega = 1.5\,\omega_{\mathrm{stand}}$.

yond a certain value, these two branches join and only solutions with relatively high summit temperature exist. It becomes clear that decreasing the heating does not necessarily favour the existence of prominence solutions. This can be understood if we imagine the behaviour of the solutions in the phase-plane. As s_h decreases, open contours turn into closed ones until after a critical value there are no more open contours and the existing contours close at intermediate temperatures and do not reach low temperatures.

The maximum allowed length and summit temperature of the hot loops decreases as a consequence of the lower heating.

6.2. Variation with area expansion rate

For constant-area loops, prominence solutions are still possible but require longer lengths. For hot loops, the area expansion works as a heating so that an increase in x leads to higher temperature summits and allows for the existence of longer loops. On the other hand, an increase of the area expansion rate is somewhat equivalent to increasing the cooling for hot-cool solutions and this allows for the existence of two branches of these type of solutions (Fig. 7). Naturally, if one increases the expansion rate even further one finds a picture similar to the one illustrated in Fig. 6d
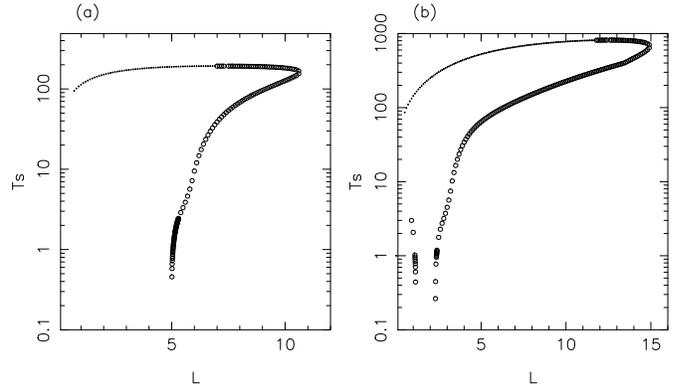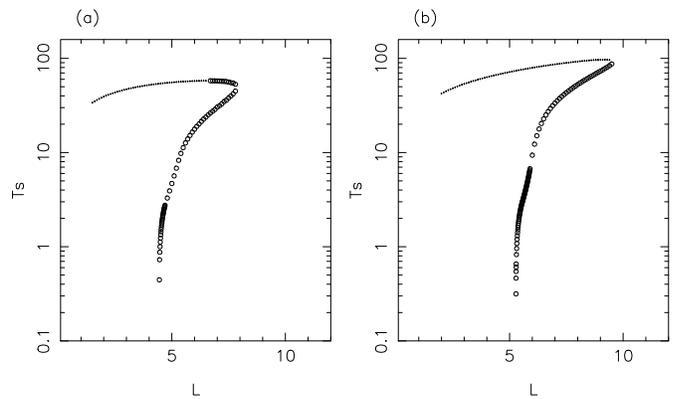
6.3. Variation with base pressure and heating

Instead of considering small departures from the base pressure or heating used in the standard case that would lead to solution diagrams similar to what we found in the preceding examples, we opt for studying different types of loops. Let us consider regions of the stellar corona characterized by a lower heating rate, lower gas pressure and therefore a lower temperature, akin to solar quiet regions. We take $h = 5 \times 10^{-8}$ and $p = 0.025$ (Fig. 8). Due to the lower gas pressure and heating, both hot and hot-cool loops have smaller maximum temperatures than in the previous sections. If the high pressure and very hot loops that have been inferred to exist in these active stars turn out not to be real then this shows that condensation solutions can still be found in large loops with more solar-like coronal temperature. This also implies that, in principle, prominences can exist in both active and quiet regions as long as an adequate magnetic field is available to support them. Let us note that due to the lower coronal temperature, the effect of gravity and centrifugal force is much more pronounced and Fig. 8b illustrates that condensation
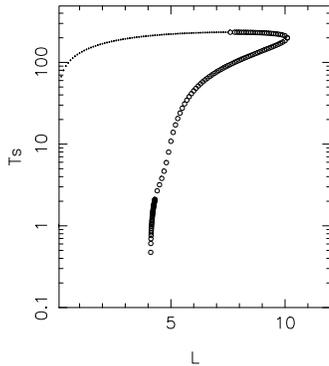
Fig. 9. The solutions dependence on the heating function: $H = h'P/T \exp(-s/s_{\rm h})$, with $h' = 2 \times 10^{-3}$ and all the other parameters are the standard ones.

solutions are possible for realistic lengths when constant heating and area are employed due the pressure increase beyond $R_{\kappa e}$.

6.4. The effect of the heating function

We now consider heating functions of different functional dependence and show that condensations can still occur.

Let us examine a form of the heating function often used in the literature, with the heating proportional to the density, $H = h'P/T \exp(-s/s_{\rm h})$. We choose $h' = 2 \times 10^{-3}$ so that with $T = 200$ and $p = 1.0$, the heating is the same as for our standard solution. The resulting diagram (Fig. 9) resembles our standard case. An interesting and somewhat intriguing feature is that the heating at the prominence region is several orders of magnitude higher than in other coronal parts of the loop due to a much higher summit density. The explanation for this apparent contradiction can be traced back to the cooling quadratic dependence on the density while the heating has only as linear dependence.

Finally, let us study the heating adopted by CC88 with $H = h'/A(s) \exp(-s/s_{\rm h})$ and impose the total heating inside the loop to be the same for different loop lengths, i.e., $H_t = \int A(s)H ds = \text{const}$. We take the total heating to be 6.7×10^{-5} and consider the other parameters to be the same as in the standard solution: $s_{\rm h} = 1.5$, $p = 1.0$, $x = 2$ (Fig. 10). Again, hot-cool loops with prominence-like summit temperatures are possible. A striking difference between this case and our standard solutions becomes apparent when we compare the flux versus length diagrams. With this heating, the hot solutions with greatest flux are not the highest but the shortest ones, and the condensation solutions are not the ones with the lowest base flux. This a direct consequence of the constraint of total constant heating for the different loops.   Although, as we have shown, this type of heating can be adopted, the analysis becomes slightly more difficult because not only the loop length, but also the base heating changes in the equations. In any case, a particular solution of the equations can equally be thought of as having either a certain amount of total heating or the respective amount of base heating. The effect of the constraint on
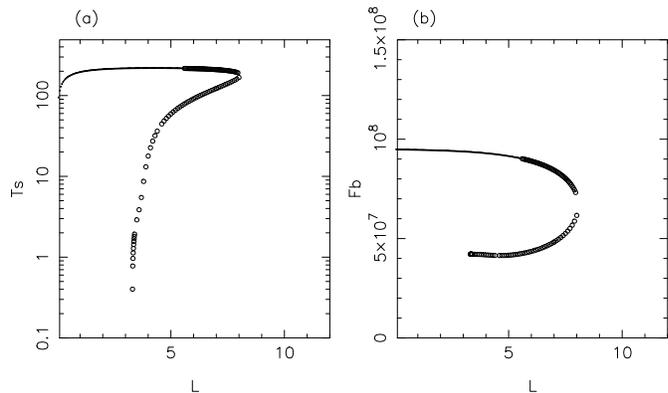

Fig. 10a and b. The solutions dependence on the heating function: $H = h'/(A(s)) \exp(-s/s_{\rm h})$ with h' determined from the constraint of constant total heating, $H_t = 6.7 \times 10^{-5}$. All the other parameters are the standard ones.

the problem has therefore in general more mathematical than physical consequences, although we find no convincing reason why short loops should have the same total amount of heating as long ones.

The type of heating functions employed, although continuous everywhere are not differentiable at the loop top. In fact, the same property is shared by the piece-wise cooling function, albeit continuous, is not differentiable. However, this has no relevant influence in the results because only the functions enter in the equations and not their derivatives.

7. The effect of asymmetries on the solutions

So far we have considered the case where all variables are symmetric with respect to the loop top. However, one can conceive many physical situations where symmetry does not exist. For example, one of the footpoints of the magnetic loop could lie in a more active region than the other from which it would result thermal energy being deposited asymmetrically along the loop. Moreover, it is certain that there are loops with different inclinations with respect to the rotation axis and this imposes an asymmetry with respect to the loop top. Although we have studied both cases, we shall only present solutions for an asymmetric heating as the results are qualitatively similar. In one case one changes the heating while in the other one changes the pressure distribution and therefore the cooling along the loop.

The equations have now to be solved from one footpoint to the other and subject to the boundary conditions

$$T_{\rm b1}(s = 0) = 0.2 \tag{17}$$

$$T_{\rm b2}(s = 2L) = 0.2 \tag{18}$$

$$p_{\rm b1}(s = 0) \quad \text{imposed} \tag{19}$$

We integrate from the first footpoint (that we refer as left footpoint) towards the second footpoint and iterate the base flux at the first footpoint until the condition $T_{\rm b2} = 0.2$ is obeyed, within an error not greater than 10%.
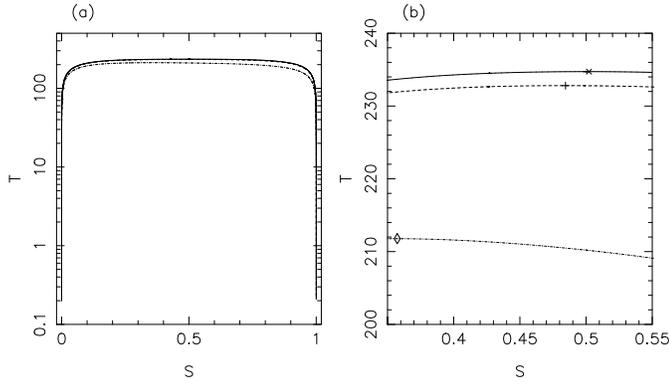
Fig. 11a and b. The effect of asymmetric heating on the Hot solutions: **a** Temperature variation; **b** Zoom of **a** near the loop summit. Shown are the solutions with symmetric heating (full line), light asymmetric heating (dashed line) and more pronounced heating asymmetry (dash-dotted line). A symbol on the different curves marks the temperature maximum.

Fig. 12a and b. The effect of asymmetric heating on the Hot-cool solutions: **a** Temperature variation; **b** Pressure variation. Solutions shown are for symmetric heating (dashed line) and asymmetric heating (full line).

To illustrate the results we consider a loop of our standard solution with $L = 3.87$, but with a modified heating function.

7.1. Hot loops

In the left leg of the loop we impose a heating function exactly the same as in the symmetric case with $h_0 = 1.0 \times 10^{-5}$ and $s_h = 1.5$. But in the other leg we choose a heating function of the form $H = h_0 \exp(-(1.95L - 0.95s)/s_h)$. At the summit the two functions match as required for continuity, while the heating in the right leg is smaller than in the left leg.

From Fig. 11 we can see that the site of the maximum temperature moves away from the summit towards the leg with more heating, as one would intuitively predict. Also shown is the more extreme case where in the loop right leg a constant heating of $H = h_0 \exp(-L/s_h)$ is deposited. In this situation the right footpoint receives about 13 times less heating than the other footpoint. Not shown is the gas pressure that is higher at the right footpoint but only by a very small amount, and this is a natural consequence of the temperature asymmetry. We note that in spite of the fact that the site of the maximum temperature moves away from the summit by a considerable distance, the maximum temperature is only slightly greater than the summit temperature. This is a consequence of the almost isothermal nature of the non-flaring hot corona, that by itself is a consequence of thermal conduction.

7.2. Hot-cool loops

Let us consider the case with the same parameters as for the hot loop with the asymmetric heating more modest. The condensation appears displaced quite considerably from the loop summit, but towards the loops leg with more heating and with a higher temperature (Fig. 12). This result is surprising and against physical intuition. At the prominence location $g_{e_\parallel} \neq 0$, a relatively large pressure gradient is necessary to support it (cf. Fig. 12).
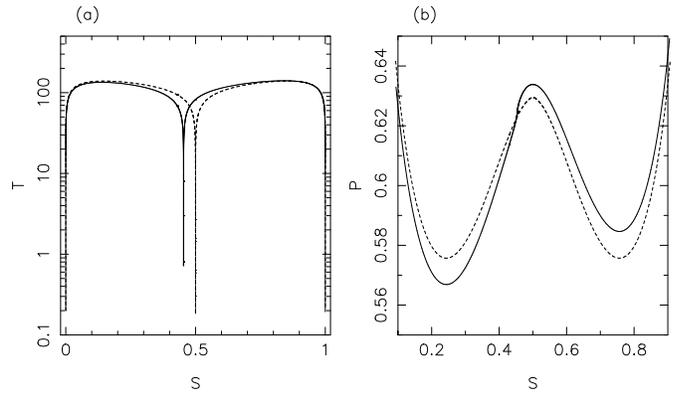
Another interesting property of this solution is the fact that the temperature maximum is located along the loop leg with lower heating. We have verified that no other hot-cool solution exists, so that this is the only static prominence solution of the energy equation for this set of parameters and boundary conditions. Furthermore, in the case of an asymmetric gravity, we find the prominence to move to the region of smaller cooling in agreement with these results.

The effect of asymmetries is complex, and to understand how it is possible to have condensations in the region with higher heating it is convenient to consider a simpler problem; the case $A = \text{const}$, $g_{e_\parallel} = 0$ and a decaying heating function. In the case of a symmetric heating distribution there are two branches of hot-cool solutions (e.g. Fig. 1) and we analyse the effect of asymmetries in the solutions of the lower branch. For a lower heating, and comparing symmetric solutions with the same summit temperature, the solutions have a larger length and base conductive flux. Alternatively, comparing solutions with the same length, a lower heating originates hot-cool solutions with a higher summit temperature. This result is counter intuitive but is a general property of the thermal equilibrium equations (cf. Sect. 6; Steele & Priest 1990). The explanation lies on the fact that the lower heating solution has a higher thermal flux at the loop footpoint.

The asymmetric solutions can be regarded as the combination of two symmetric solutions with the same summit temperature but with different heating distributions, one with the same length and heating as the symmetric case and another with a longer length but smaller heating. Therefore, the resulting asymmetric solution has a condensation in the loop leg with a higher heating and its temperature is higher than in the symmetric case (from the point of view of any of the two symmetric solutions, the condensation appears at a distance from the footpoint shorter than their half-length).

Symmetric solutions of the upper branch with a lower heating rate have a smaller length and base conductive flux for the same summit temperature. Consequently, one finds that the op-
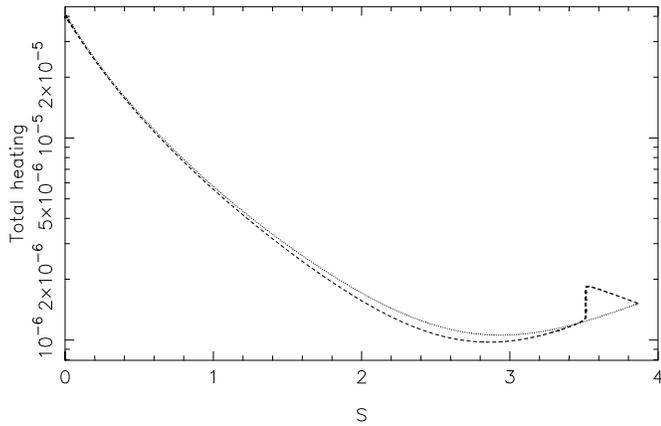
Fig. 13. The total heating along the loop from the footpoint to the summit. The left loop leg is shown as a dashed line and the right leg as a dotted line.

posite happens, i.e., the condensation appears in the leg with less heating.

These properties generalise to loops in the presence of gravity, but are not applicable to loops with non uniform cross-sectional area. The presence of an area variation introduces an effective extra heating term, positive or negative, that has the ability of changing the total heating distribution along the loop. For the standard solution, the total heating is actually greater along most of the loop leg with a lower heating deposition than along the leg with a higher heating (Fig. 13) and this explains our result above shown in Fig. 12. We have also studied the effect of asymmetries in our standard hot-cool loops with high summit temperature. We find that there are three different hot-cool solutions. Two of them have their local temperature minimum along the loop leg with lower heating, while the other has it on the other side of the loop. As one moves towards loops of shorter length and smaller temperature one finds that the two solutions that have their temperature minimum on the same loop leg approach each other until they merge and disappear and only the solution with the temperature minimum along the loop leg with higher heating lasts. The physical reason for the non-existence of a condensation solution in the loop leg with lower heating is that in the presence of an area variation the total heating asymmetry becomes too high for it to exist.

In any case the solutions obtained are probably dynamically unstable as they lie away from the loop summit. A possibility is that our model lacks physical content. If the plasma is optically thick, the width and mass of the cool region are increased, and not only the energy but also the momentum balance is changed. This could modify the location where we find the prominence in a significant way. If one maintains the assumption that the plasma is optically thin, then we suggest, following Antiochos & Klimchuk (1991), that there is a prominence solution at the loop summit that could be stable, yet not in a static equilibrium but rather in the presence of small steady plasma flows (cf. Appendix A).

8. Discussion

The results obtained allow us to interpret and question some conclusions of other authors who addressed similar problems. CC88 concluded that in order to explain the existence of very large loops it is necessary that the loop cross-sectional area does not vary with distance from the star more strongly than $A \sim r/R_\star$. However, this a direct consequence of the heating function adopted: $H = h/A(s) \exp(-s/s_h)$ with the total heating constant for loops with different expansion rates and lengths. In fact, considering loops with higher expansion rates leading to a heating function decreasing faster with height, which is equivalent in our formulation to consider a low value of s_h, and this decreases the maximum height of equilibrium solutions (cf. Fig. 6). Bearing in mind that little is known about the heating mechanisms of the corona, it is not acceptable to make such a strong conclusion that is so dependent on the form of the heating function. Furthermore, even if there are no long hot loop solutions of the static equilibrium equations, one can always interpret the X-ray observations in terms of non-static loops. Van den Oord & Zuccarello (1996) claim that the temperature inversion solutions obtained by CC88 in the constant cross-sectional case are not possible. However, we have shown that if the heating decreases towards the summit this induces the appearance of condensation type solutions without the need for expanding loops (cf. Sect. 6.2) and we conclude that this type of solutions is real. Naturally, one expects the field strength to decrease with height so that some degree of expansion occurs but we have shown that there is no need for very fast expanding loops to find condensation solutions. Furthermore, the centrifugal force can have a similar effect in inducing the existence of these type of solutions if the loop temperature is typical of solar non-flaring regions but not if it is as high as it has been suggested ($T \sim 10^7$ K).

In this study we have favoured a heating that decreases along the field although we have also shown that this is not a necessary condition for the existence of condensations. This type of heating is physically acceptable. For example, if the corona is heated by waves one expects them to dissipate energy along their path. This results in a decaying heating towards the summit, the particular form depending on the exact mechanism that extracts energy from the waves. On the other hand, if the heating results from small-scale reconnecting events then a heating of this type could result if the energy is released closer to the footpoints.

Ideally, we would like to find out whether the different types of solution we have obtained are stable because only then we would know that they are attainable in nature. Some of the prominence solutions presented lie below $R_{\kappa e}$ and are therefore subject to the Rayleigh-Taylor instability, although one could easily consider a magnetic loop with a summit convex with respect to the surface that would invalidate this particular type of instability. The hot-cool solutions obtained in the presence of asymmetries seem unlikely to be dynamically stable, but a proper stability analysis is required to confirm this. CC88 provided an analysis of the stability of the hot and hot-cool solutions. Unfortunately a perturbed energy equation was

derived considering a temperature variation with all other physical quantities remaining constant (i.e. pressure, density and velocity). One can easily verify that none of the other equations, i.e. momentum, mass conservation and state, is obeyed. Therefore, no valid conclusions can be inferred from this work. In a classical paper, Field (1965) clarifies the physics of thermal instability. For a loop with a coronal temperature we find for the radiative cooling time, $\tau_r \approx$ several days, while the sound travel time for a loop of half-length $3\,R_\odot$ is $\tau_s \approx 1$ hour. Therefore, sound propagates almost instantaneously on the time-scale of temperature evolution and one can ignore the inertial term in the perturbed linear momentum equation. We expect some, if not all, hot-cool loops with high summit temperature to be unstable. Let us consider a local analysis at the loop top. Here $A \approx$ const and $g \approx 0$ so that $p_0 =$ const and $p_1 =$ const and we take $p_1 = 0$. Writing any physical variable as

$$f(s,t) = f_0(s) + f_1(s)\exp(\sigma t), \qquad f_1(s) \ll f_0(s) \qquad (20)$$

and considering long-wave temperature perturbations so that

$$\frac{1}{T_1}\frac{dT_1}{ds} \ll \frac{1}{T_0}\frac{dT_0}{ds}, \qquad (21)$$

we can neglect derivatives of T_1 and the energy equation for a plasma with $\gamma = 5/3$ can be written as

$$5R\rho_0\frac{DT}{Dt} = T_1\left\{-\frac{d}{ds}\left(K_0\frac{d}{ds}\left(T_0^{\frac{5}{2}}\right)\right)\right.$$
$$\left. + \rho_0^2\left(2\frac{Q(T_0)}{T_0} - \frac{dQ}{dT}\right)\right\}. \qquad (22)$$

In the region of temperature inversion, the conductive term, $-d(K_0 d(T_0^{5/2})/ds)/ds)$, is always positive and so is the radiative term for $T > 1.5 \times 10^4$ K. The temperature of an element of volume will therefore vary so as to increase the temperature perturbation, i.e., towards instability. This indicates that hot-cool loops with summit temperatures not too low are probably unstable although a proper stability analysis is required to confirm this simple estimate.

If we take as an indicator the results on the stability of hot solar coronal loops, we expect short hot loops to be stable due to the influence of gravity (Wragg & Priest 1982; Klimchuk et al. 1987), while long ones could be unstable due the influence of the centrifugal force in increasing the destabilizing effect of the radiative cooling.

Many of the loops we have considered here are extremely long requiring very high magnetic field strengths to contain the plasma. Our assumption of magnetic rigidity certainly breaks down, and a limit on the maximum height of quasi-static coronal loops is more likely to come from lateral force balance constraint than from energy balance.

Although we have shown that prominence solutions exist, we have not addressed the question of how they become available. Van den Oord & Zuccarello (1996) state that the presence of cool material is possible without the need of a thermal instability. But this assertion seems to miss the whole point.

Just because static solutions of the equations exist describing prominences, one has to realise that prominences have a finite lifetime. Therefore, there must be a dynamical transition from one state (most likely a hot one) to a prominence like structure which is likely to involve some sort of thermal instability or non-equilibrium. The injection mechanisms proposed to supply mass to solar prominences (e.g. An et al. 1988) are very unlikely to be important for their stellar counterparts due to the large lengths involved. In a more natural scenario, a change in heating, pressure or loop length could drive a hot loop thermally unstable. As the instability develops, the plasma is driven by a siphon flow from the stellar surface towards the prominence location where the plasma condenses to form a prominence (Pikel'ner 1971).

Jefferies (1993) proposed an attractive model in which X-ray flares and prominences are at the same time cause and consequence of each other. He considers a scenario akin to two-ribbon solar flares and the associated post-flare loops as first proposed by Kopp & Pneuman (1976) and extended thereafter by several authors (e.g. Kopp & Poletto 1984; Forbes & Malherbe 1986). During a flare the open magnetic field lines continually reconnect to form closed field lines. At the reconnection site, large amounts of energy are released and fast particles accelerated, that together evaporate chromospheric material that feeds the newly formed loops with very high temperature and density X-ray plasma. As the heating decreases, the plasma cools to form a prominence. Contrary to solar loop prominences that are short lived and for which the cool plasma drains to the surface, in sufficiently high stellar loops, due to the centrifugal force, plasma can remain at or close to the loop apex to form a quiescent prominence. It is, however, necessary that the plasma is thermally stable or otherwise it evaporates by thermal conduction down to the chromosphere. Our models presented here represent this type of prominences after a steady and static state is reached. As the reconnection proceeds, the X-neutral point continually reforms at higher altitudes creating more and more closed loops and leading to a growth of the size of the prominence. This system would evolve until a point where the magnetic field could not sustain the plasma leading to an eruption and a new flare. The whole process could, in principle, repeat itself.

Although this constitutes a plausible picture, there is still little observational evidence to indicate such a close association between prominences and large X-ray flares. A different, but closely related, scenario is one in which an increase of the heating at the loop base caused by, for example, small-scale flaring evaporates chromospheric plasma into the coronal part of the loop. This would drive an increase of the density that could trigger a thermal instability and lead to the formation of a prominence. A similar mechanism has been investigated by Antiochos & Klimchuk (1991) to explain the formation of solar prominences.

9. Conclusions

We have determined the thermal structures of large coronal loops on rapidly rotating stars. We find two types of equilibrium solutions. There are loops with a temperature maximum

at the summit and others with a local temperature minimum. The former ones have coronal temperatures over most of their lengths, while the latter ones can have summit temperatures from coronal values down to prominence like temperatures.

If stellar prominences can be considered as globally static structures, then there must be a solution of the static energy and momentum equations representing them. With this idea in mind, we determined the properties of prominence solutions and explored their dependence on the different parameters. Generally, varying the parameters as to decrease the heating, or increase the cooling, favours their existence. However, if the heating is very small, then there are no prominence solutions available. We have also proved that prominence type solutions are possible for a wide range of heating functions and parameters. In particular, we find that there is no need for very rapidly expanding loops. We were lead by the observations to consider loops with a gas pressure similar to the one found in solar active regions, but we have also shown that prominences can exist in quiet regions characterised by a much lower gas pressure, coronal temperature and heating.

The presence of an asymmetry in the heating or cooling causes the prominence to move away from the summit in the direction of higher or lower heating depending on the parameters of the problem. We suggest that these solutions are unstable and that prominences should exist at the loop summit and show that this is indeed possible in the presence of small plasma flows.

In the future, determining the relation between X-ray flares and stellar prominences as well as the connection between prominences and underlying surface magnetic features, such as spots and plages, will lead to a better understanding of the conditions necessary to prominences formation. On the theoretical side, efforts should be directed in determining the conditions for which hot loops can become thermally unstable as well as clarifying the effects of asymmetries in the problem. The dynamical processes involved should also be addressed in order to constrain the possible mechanisms of prominence formation and evolution.

Appendix A: prominence solutions in the presence of small-scale steady flows

In order to support the suggestion that a hot-cool solution can be found in the loop summit when the heat distribution is not symmetric, we solve the steady-state energy, mass conservation and momentum equations for a $\gamma = 5/3$ gas

$$\frac{dF_c}{ds} = A\xi \left(p^2 \chi T^{\alpha-2} - H \right) - A\Theta \left(v\frac{dp}{ds} - \frac{5}{2}v\frac{p}{T}\frac{dT}{ds} \right) \quad \text{(A1)}$$
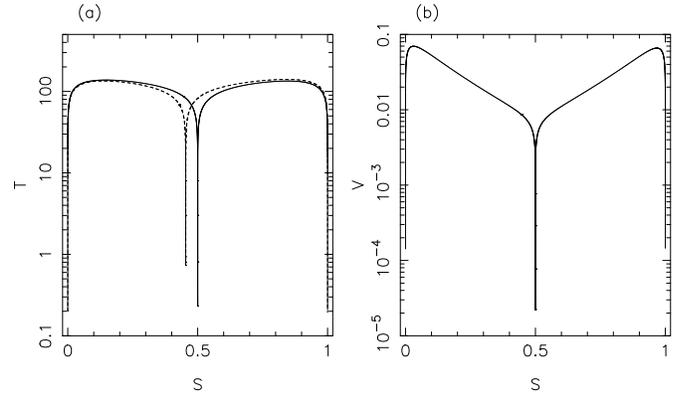

Fig. 14. a The temperature profile for the static loop of Sect. 7 (dash line) and the loop with a steady flow and $L = 3.73$ (solid line); **b** The velocity along the loop in units of C_{s_0}.

$$v = v_b \left(\frac{p_b}{p} \right) \left(\frac{T}{T_b} \right) /A \quad \text{(A2)}$$

$$\frac{p}{T}v\frac{dv}{ds} = -\frac{dp}{ds} + \frac{p}{T}g, \quad \text{(A3)}$$

with the dimensionless parameter $\Theta = R_* C_{s_0} p_0 / K_0 T_0^{\frac{5}{2}}$ and the suffix b representing a given quantity at the left footpoint.

We consider the same parameters of Sect. 7 with the velocity defined in units of the isothermal sound speed $C_{s_0} = \sqrt{2RT_0}$. For $L = 3.87$, the hot-cool solution in the presence of a flow has a summit temperature $T_s = 1.65$ which is too high to resemble a prominence temperature. Nevertheless, by considering other loop lengths one can find hot-cool solutions with small summit temperatures. A particular case is shown in Fig. 14 where a small plasma flow from the right to the left footpoint, i.e., towards the footpoint on the more heated side changes the energy distribution along the loop and moves the condensation to the loop summit. The maximum flow speed is $v_{max} \approx 4 \, \text{km s}^{-1}$ and its direction is opposite to the one required to move the maximum temperature of the hot solution to the loop summit. The strong acceleration and deceleration present close to the footpoints and the prominence is a consequence of mass conservation. Nevertheless, the pressure has a smooth behaviour because the velocities present are very small.

In the energy equation the enthalpy flux was found to be the relevant new term with a negligible contribution from the term due to gas pressure variations. Naturally, the direction of the flow does not depend on whether the static solution has the condensation along the loop leg with more or less heating, as it only works to balance the heating asymmetry and because the area variation heating contribution is very close to symmetric when the condensation is at the summit. Between the loop footpoint and the temperature maximum the enthalpy flux works as an extra cooling in the right leg and as a heating in the left leg. Recalling that in the static case the maximum temperature is located along the right leg, then we understand that this has the effect of approximately equalizing the maximum temperature of the two loop legs. On the other hand, between the temperature

maximum and the summit the enthalpy flux works as a heating in the right leg and as a cooling in the left leg and therefore reestablishes the heating deficit in these parts of the loop.

We have also computed the static and non-static thermal equilibrium of a loop with typical solar parameters (semicircular loop of constant area with a semi-length of 19 Mm and with a spatial dependent heating function) and found the same behaviour. We cannot rule out the possibility that for some parameters the contribution to the energy equation of the pressure gradient term supersedes the enthalpy flux and in this unlikely situation the flow would be in the opposite direction.

Antiochos & Klimchuk (1991) simulated the time-dependent formation of a solar prominence in the presence of an asymmetric heating. They observe that a condensation starts to form in the region where the heating is smaller, away from the loop midpoint. Unfortunately, the code breaks down before reaching a steady state. They argue, however, that a final steady state would be reached with a prominence at the loop summit in the presence of a flow from left to right. By actually solving the steady state problem we have shown that this scenario is possible but the flow is generally in the opposite direction to their prediction.

References

An C.-H., Bao J. J., Wu S. F., 1988, Solar Phys., 115, 81

Antiochos S. K., Klimchuk J. A., 1991, ApJ, 378, 372

Antiochos S. K., Noci G., 1986, ApJ, 301, 440

Collier Cameron A., Bedford D.K., Rucinski S.M., Vilhu O., White N.E., 1988, MNRAS, 231, 131

Collier Cameron A., Robinson R. D., 1989a, MNRAS, 236, 57

Collier Cameron A., Robinson R. D., 1989b, MNRAS, 238, 657

Collier Cameron A., 1988, MNRAS, 233, 235, (CC88)

Collier Cameron A., 1996, in Strassmeier K., Linsky J., eds, IAU Symposium 176, Stellar Surface Structure. Kluwer Academic Publishers, p. 449

Cook J. W., Cheng C.-C., Jacobs V. L., Antiochos S. K., 1989, ApJ, 338, 1176

Cox D. P., Tucker W. H., 1969, ApJ, 157, 1157

Field G. B., 1965, ApJ, 142, 531

Forbes T. G., Malherbe J. M., 1986, ApJ, 302, L67

Hildner E., 1974, Solar Phys., 35, 123

Hood A. W., Anzer U., 1988, Solar Phys., 116, 61, (HA)

Hood A. W., Priest E. R., 1979, A&A, 77, 233

Jefferies R. D., 1993, MNRAS, 262, 369

Klimchuk J. A., Antiochos S. K., Mariska J. T., 1987, ApJ, 320, 409

Klimchuk J. A., Lemen J. R., Feldman U., Tsuneta S., Uchida Y., 1992, PASJ, 44, L181

Kopp R., Pneuman G., 1976, Solar Phys., 50, 85

Kopp R., Poletto G., 1984, Solar Phys., 93, 351

Kuin N. P. M., Poland A. I., 1991, ApJ, 370, 763

Martens P. C. H., Kuin N. P. M., 1982, A&A, 112, 366

McClymont A. N., Canfield R. C., 1983, ApJ, 265, 497

Mendoza C. A., Hood A. W., 1996, Astro. Lett. and Comm., 34, 107

Mendoza C. A., 1996, PhD thesis, University of St. Andrews, St. Andrews, Scotland

Pikel'ner S. A., 1971, Solar Phys., 17, 44

Raymond J. C., Smith B. W., 1977, ApJS, 35, 419

Rosner R., Tucker W. H., Vaiana G. S., 1978, ApJ, 220, 643, (RTV)

Serio S., Peres G., Vaiana G. S., Golub L., Rosner R., 1981, ApJ, 243, 288

Sptizer L., 1962, Physics of Fully Ionized Gases. Interscience, New York

Steeghs D., Horne K., Marsh T. R., Donati J. F., 1996, MNRAS, 281, 626

Steele C. D. C., Priest E. R., 1990, Solar Phys., 125, 295

Steele C. D. C., Priest E. R., 1991, Solar Phys., 132, 293

Steele C. D. C., Priest E. R., 1994, A&A, 292, 291

Steinolfson R. S., van Hoven G., 1984, ApJ, 276, 391

Unruh Y. C., Jardine J., 1996, A&A, in press

van den Oord G. H. J., Zuccarello F., 1996, in Strassmeier K., Linsky J., eds, IAU Symposium 176, Stellar Surface Structure. Kluwer Academic Publishers, p. 433

Vesecky J. F., Antiochos S. K., Underwood J. H., 1979, ApJ, 233, 987

Wragg M., Priest E. R., 1982, Solar Phys., 80, 309